

TANGENTIAL LEADING-EDGE BLOWING ON A COMBAT AIRCRAFT CONFIGURATION

by
*D G Mabey, Visiting Professor, Dept of Aeronautics,
 Imperial College, London, UK*
 and
*C R Pyne, Senior Scientific Officer, Defence Research Agency,
 Aircraft Section, Bedford, UK*

Summary

Tangential leading-edge blowing on the inboard strake was used to control the flow separations developing on a large half model of the Experimental Aircraft Project (EAP) configuration. Significant improvements in overall force characteristics (increases in lift and decreases in drag) were observed, together with useful reductions in fin buffeting, which is used as the control during the experiment. The reductions in wing buffeting were less noticeable than for the fin. The values of jet momentum coefficient required were somewhat smaller than in previous tests on smaller models at lower Reynolds numbers. Changes in steady and fluctuating pressure distributions close to the slot and across the span together with flow visualisation using minitufts indicate how the overall aerodynamic characteristics of the wing were modified by blowing limited to the strake.

List of Symbols

C_{BF}	fin static bending moment coefficient
\bar{c}	wing aerodynamic mean chord(0.868 m)
C_p	pressure coefficient
$\sqrt{nG(n)}$	buffet excitation parameter
m	generalised mass
$n = \bar{f}\bar{c}/U$	frequency parameter
$\sqrt{nF(n)}$	rms level of excitation at frequency parameter n
\bar{p}	broad band rms pressure
$q = \frac{1}{2}\rho U^2$	free stream kinetic pressure
R	Reynolds number based on \bar{c}
x	streamwise co-ordinate
y	spanwise co-ordinate
\ddot{z}	rms tip acceleration in mode
U	free stream velocity
α	incidence
ζ	total damping, fraction of critical
$\eta = y/S_w$	semi-span ratio

Introduction

Previous tests⁽¹⁾ and calculations⁽²⁾ have shown that tangential leading-edge blowing through a narrow slot can reduce or suppress leading-edge separation on delta wings with round leading edges. This improves the overall steady force characteristics and reduces the wing and fin buffeting. However, generally such tests were confined to small models (sometimes tested with free transition) and low speeds, giving low Reynolds numbers and transitional boundary layers. In addition many of the tests were made on wings with unrealistic sections eg delta planforms with constant thickness.

In an attempt to remedy these deficiencies, some comprehensive tests⁽³⁾ were made on a large half model of the RAE High Incidence Research Model (HIRM1) configured to represent the Experimental Aircraft Project (EAP) Fig 1). This allowed a careful assessment of the blowing requirements for a practical configuration, albeit with blowing limited to the leading-edge strake. These tests were made with fixed transition over the Reynolds number range from 2.5×10^6 to 4.3×10^6 ($U = 40$ m/s to 70 m/s). Unless otherwise stated the results presented relate to $R = 3.7 \times 10^6$ ($U = 60$ m/s).

This report summarizes the salient results from these tests⁽³⁾. The momentum blowing coefficient has been estimated, and varied in four ways: by varying the blowing pressure, the stream velocity, the slot area and the slot taper ratio. The tests comprise measurements of steady overall forces, steady and fluctuating pressures on the wing, together with buffeting on the fin (which is used as the control parameter during the experiment) and the wing. In addition, mini-tuft photographs have been used to infer the general character of changes in the development of the viscous flow over the whole wing as slot blowing is applied at the leading edge of the strake.

The general conclusion is that significant improvements in aerodynamic performance can be obtained for lower values of momentum coefficient than suggested by the previous tests on small models. Thus the

Copyright © 1994 by the United Kingdom Government.
 Published by the American Institute of Aeronautics and
 Astronautics, Inc. with permission. Released to ICAS/AIAA
 to publish in all forms.

concept of tangential leading-edge blowing to control flow separation could be considered seriously in any future project studies

Experimental Details

The large half model of the HIRM in the configuration of a 1/3.8 scale model of the EAP aircraft was described fully elsewhere⁽³⁾. Hence for brevity only the special features pertinent to the blowing tests are described here.

Blowing Arrangements

Blowing air was supplied from a high pressure storage vessel at 20 bars and controlled by a throttle valve (Fig 2a). The method used to compute the momentum coefficient, C_{μ} , is described elsewhere⁽³⁾. The leading edge region was modified to allow the slot configuration to be adjusted rapidly. The insert (Fig 2b) provided a tangential jet of air from a narrow slot at the leading-edge chord line of the strake. This was tested with the following settings:

- (a) Slot tapering linearly from 0 at the root of the strake to 1 mm at the end of the strake,
- (b) Uniform slot width of 0.5 mm (same area as (a)),
- (c) Uniform slot width of 1 mm (twice area of (a)).

Fin and Tip Pod

With the leading-edge blowing restricted to the strake, it was recognised that the reductions in wing buffeting in the first bending mode were likely to be small. (In this mode the section of the wing outboard of the kink makes the largest contribution to the forcing). However, leading-edge blowing on the strake was expected to apply a powerful control to the flow separations inboard on the wing, thus affecting the wake region, where a fin might be fitted on a typical combat aircraft. Accordingly an F-18 style fin, which had been used in previous buffeting tests, was fitted for most of the present blowing tests (Fig 3a). Manifestly, the mode shape and excitation field on this fin were different from those appropriate to the wing, yet some degree of commonality could be provided by ensuring the same frequency on both components. Thus, for a given velocity, the same frequency parameter was obtained for both modes emphasizing the differences due to the mode shapes and the excitation fields. There is no significant mechanical coupling between the wing and fin motions. The wing and fin first bending frequencies were 22 Hz and 33 Hz respectively. Accordingly the fin first bending frequency

was lowered to 22 Hz by the addition of tip pod of mass 168 g (Fig 3b) (giving values of $n = 0.32$ and 0.48 respectively at $U = 60$ and 40 m/s). With this simple modification, the fin became a sensitive indicator of the degree of control achieved by blowing on the leading edge of the strake. Thus the fin-root strain signal could be used as the "control-parameter" during the main series of tests.

Instrumentation and Analysis

Two separate systems were used for these measurements. The forces and moments on the model were measured by the half-model balance and recorded by the tunnel computer, using the standard balance matrix. The steady and time-dependent measurements on the model (of wing pressure, wing-tip acceleration, fin-root strain and temperature) were measured independently of the force data by an updated version of the RAE Presto high-bandwidth digital data acquisition system. The Presto system was used to compute the static pressure coefficient, C_p , the rms levels, \overline{p}/q , and the spectral

levels, $\sqrt{nF(n)}$ according to the standard AGARD notation given by Owen⁽⁴⁾. Most of the transducers were located at the sections with $\eta = 0.4, 0.6$ and 0.8 at fairly wide intervals. However, to provide some indication of local conditions close to the blowing slot additional pressure transducers were inserted at $\eta = 0.5$ at $x = 0.01, 0.02, 0.03, 0.04$ and 0.05 (cf Fig 1).

Analysis of the fin-root strain signal was particularly important, because this was used as the "control parameter" during the main series of tests. The DC level gave the static fin bending moment coefficient,

$$C_{BF} = \frac{\text{Moment}}{qS_F s_F}, \quad (1)$$

where q = kinetic pressure,
 S_F = fin area (0.165 m^2)
 and s_F = fin semi-span (0.522 m).

The unsteady component at 22 Hz was used to compute the fin buffet excitation parameter, $\sqrt{nG(n)}$, according to the relation

$$\sqrt{nG(n)} = \frac{2}{\sqrt{\pi}} \left[\frac{m\ddot{z}}{qS_F} \right] \zeta^{1/2}, \quad (2)$$

where m = generalised mass in the mode,

\ddot{z} = fin tip acceleration in the mode,
and ζ = total damping fraction critical.

An expression similar to equation (2) was used to calculate the buffet excitation parameter in the wing first bending mode.

Test Conditions

A 3 mm wide band of ballotini, 0.36 mm in diameter was applied to fix transition on both the wing and the fin (Fig 1) at velocities at and above 40 m/s. The test velocities were generally 40 and 60 m/s, but a few measurements were made at 70 m/s. For these special tests the fin was removed to avoid damage due to the high amplitude vibrations which would have been experienced at high angles of incidence. The tests were made in August 1992.

Results

Without blowing these slot configurations can be added to the leading-edge of the strake without significantly altering the overall aerodynamic characteristics of the configuration⁽³⁾. For a given slot configuration there are no large scale effects (as between velocities of 40, 60 and 70 m/s) on the values of the momentum coefficient, C_{μ} , required to reduce the fin and wing buffeting to the minimum levels which can be achieved for a given angle of incidence. Manifestly the leading-edge separation is being controlled by C_{μ} at these high Reynolds numbers, as it was in earlier tests at low Reynolds numbers^(1,2). In addition a comparative assessment shows that for a given value of C_{μ} , the three different slot configurations show the same characteristic effects. Hence it is convenient to discuss the effects of leading-edge blowing on the tapered slot at $R = 3.7 \times 10^6$ as a function of the angle of incidence. The small variations between the three slot configurations are described elsewhere³.

Influence of Strake Slot Without Blowing

A pre-requisite for the success of modifying an existing aircraft (such as the EAP) to incorporate leading-edge blowing would be that the addition of the narrow blowing slot should not modify adversely the overall aerodynamic characteristics. The changes in the overall forces are small (at least for the low speeds characteristic of subsonic flow) and there appears no *a priori* aerodynamic reason why a blowing slot of a width of about 4 mm should not be incorporated into this type of combat aircraft with a round leading edge. However,

there might be formidable engineering problems.

Choice of Blowing Momentum Coefficient (C_{μ})

The unsteady fin-root strain signal was used as the prime control parameter. Fig 4 shows typical results for $\alpha = 15^\circ, 20^\circ, 25^\circ$ and 30° . For a given angle of incidence, the steady bending moment coefficient, C_{BF} , increases steadily with C_{μ} and then generally tends towards a constant level (Fig 4a). This suggests that the principal effect of blowing is the downward displacement of the strake vortex, inferred from the vortex motions observed previously. The unsteady fin-root strain signal,

represented as $\sqrt{nG(n)}$, decreases steadily with C_{μ} until a minimum value is obtained (Fig 4b). This minimum value is selected as the optimum momentum

coefficient, C_{μ} for blowing. Thereafter $\sqrt{nG(n)}$ increases with C_{μ} . The rate of increase is slow up to and including $\alpha = 25^\circ$ but rapid at $\alpha = 30^\circ$. The initial decrease in fin buffeting is due to the downward displacement of the strake vortex (related with the increase in C_{BF}) and a decrease in the strength of that vortex. The subsequent increase comes from increases in the excitation which are most noticeable outboard of the strake. We shall see this illustrated clearly on the wing for $\alpha = 30^\circ$ at $\eta = 0.6$ (Fig 7c) and 0.8 (Fig 7d). The

wing-tip acceleration, also represented as $\sqrt{nG(n)}$, shows similar, but less obvious variations to the fin (Fig 4c). This is because for wing bending the most effective excitation is at the wing-tip. In the tip region the flow is less affected by blowing on the strake than at the wing-root. Hence the initial reductions in buffeting (due to the reduction of strake separations) are less obvious on the wing. The optimum value of C_{μ} found for the fin generally corresponds with a minimum value for the wing buffeting (cf Figs 4c & 4b).

The principal effect of tangential leading-edge blowing is to reduce the wing effective incidence, thus lowering the position of the centre of the wing separations, which is crucial to the fin buffeting. However, in addition to this reduction in height, blowing on this wing has two other effects (Fig 4d). The first is a **small inboard displacement** of the reattachment line (cf subsequent discussion of Fig 8a). The second is a general lowering of the level of excitation consequent upon the reduction in the overall scale of the separations. A similar lowering of the excitation follows the reduction of the

overall scale of the separation due to a reduction in the angle of incidence for wings without blowing (Fig 4e).

Having selected the optimum values of C_{μ} , a direct comparison can be made of the control parameters with the blowing on and off (Fig 5). While the changes in static C_{BF} are fairly small (Fig 5a), the reduction in fin buffeting is significant (Fig 5b) whereas the reductions in wing buffeting are quite small at $\alpha = 20^\circ$ and 30° and negligible at $\alpha = 25^\circ$ (Fig 5c). Fig 6 shows that these optimum values of C_{μ} are not sensitive to changes in the slot configurations, the stream velocity, the blowing velocities or the presence of the fin.

The static values of fin-root strain (represented as C_{BF} in Fig 5a) should have important implications with respect to the lateral stability of an aircraft. This is because without blowing, as α increases the loss in C_{BF} due to the upward and inward movement of the wing flow separations is associated always with a loss of fin and rudder effectiveness. It is reasonable to expect that the positive increments in C_{BF} due to blowing (even at $\alpha = 30^\circ$) will be associated with some recovery of fin and rudder effectiveness. Although this cannot be verified on this half model it has been demonstrated on smaller complete models during tests at low Reynolds numbers

The changes in the overall forces and moments associated with the optimum blowing coefficients are small and differ little between two typical slot configurations. These integrated forces and moments are thus consistent with the small changes in the pressure distributions between the different slot configurations. There are two significant changes due to blowing. The first is the increase in lift coefficient of about 0.1 at $\alpha = 30^\circ$ associated with the delay in the breakdown of the strake vortex. The second is the decrease in the drag coefficient observed, which is sometimes about 0.02.

Influence of Blowing on Wing Pressure Distributions

As an illustration of the results given in Ref 3, the steady and fluctuating pressure distributions on the wing are presented for the tapered slot without blowing and with the optimum value of C_{μ} for $\alpha = 30^\circ$. It is convenient first to consider the pressures very close to the blowing slot (for $\eta = 0.5$, $x/c = 0.01$ to 0.05) before considering the pressures on the strake (for $\eta = 0.4$) and outboard of the strake (for $\eta = 0.6$ and 0.8).

Fig 7 shows the pressure distributions. Here the burst point of the strake vortex has moved well forward, towards the apex of the wing. Hence it has little influence

on the large scale bubble separations outboard of the kink. The major effect of blowing on the overall forces is an increase in lift coefficient attributed to the displacement of the vortex burst downstream from the apex. As for all the lower angles of incidence, very close to the slot (Fig 7a) blowing increases the local suction and the excitation. The steady suctions are increased by the reduction in speed from $U = 60$ to 40 m/s but there is a marked reduction in the local excitation.

For $\eta = 0.4$ (Fig 7b) blowing increases both the suctions and the excitation (apart from a minor anomaly at $x/c = 0.8$): There is a local increase in excitation whilst the fin buffeting is reduced. For $U = 40$ m/s the steady pressures are much the same but the fluctuating pressures vary somewhat. Without blowing the excitation is the same as at $U = 60$ m/s, whereas with blowing the excitation is significantly lower, implying a more effective local control of separation at the lower Reynolds number.

For $\eta = 0.6$ (Fig 7c) the changes in the pressure distribution due to blowing extend from the leading edge to about $x/c = 0.6$: over this region there is a marked increase in excitation due to blowing. For $U = 40$ m/s the steady and fluctuating pressure distributions without blowing are identical. However, with blowing the suctions are appreciably higher and the region of high excitation is displaced downstream, with a maximum at about $x/c = 0.6$. Both these observations suggest a more effective control of separation at the lower Reynolds number.

For $\eta = 0.8$ and $U = 60$ m/s (Fig 7d) there is only a small increase in suction when blowing and there is an increase in excitation upstream of $x/c = 0.5$. This increase in excitation is apparently inconsistent with the small reduction in wing buffeting observed. However, we must remember that \bar{p} represents an rms pressure fluctuation and that \bar{p} can increase at high frequencies (due to entrainment) and yet have a lower level at $f = 22$ Hz (the wing first bending frequency). For $U = 40$ m/s the steady and fluctuating pressures are the same as at 60 m/s without blowing. However with blowing both the suctions and the excitations are higher. These observations probably imply greater entrainment and more effective control of separation at the lower Reynolds number.

Influence of Blowing on the Mini-tuft Observations

These observations are summarized in Fig 8 for a velocity of $U = 60$ m/s (the results for $U = 40$ m/s are much the same). Previous research confirms that of the

mini-tufts give an indication of the general development of the three-dimensional viscous flow.

For $\alpha = 15^\circ$ (Fig 8a) the wing flow is dominated by a swept bubble which forms on the wing apex and the outboard section. This swept bubble is characterised by a strong spanwise flow without the clearly marked point of inflection associated with a tightly rolled vortex. With blowing the main change in the mini-tuft photographs is that the "foot-print" of the swept bubble becomes larger, making the area of attached flow at the root appreciably smaller. In addition the spanwise flow under the bubble is reduced a little. With blowing, the bubble probably has a different shape and may have reduced circulation. Then these combined effects would explain the reduction in excitation observed⁽³⁾ at $\eta = 0.4$ and at $\eta = 0.6$. The only difference in the minituft observations at $U = 40$ m/s is that the "foot-print" of the swept bubble is somewhat larger at the lower speed consistent with larger viscous effects at the lower Reynolds number. With $\alpha = 15^\circ$ the wing has only light buffeting where previous research suggests significant scale effects would be expected.

For $\alpha = 20^\circ$ (Fig 8b) again the wing flow is dominated by a swept bubble, which is larger than at $\alpha = 15^\circ$. With blowing the main change is around $\eta = 0.4$ where the tufts are steadier. In addition, in this region near to the leading edge the tufts are close to the streamwise direction whereas further downstream the outward spanwise flow under the bubble is less marked. For $U = 40$ m/s the changes around $\eta = 0.4$ are similar in character (albeit less obvious), consistent with small scale effects with the larger separation, as expected.

For $\alpha = 25^\circ$ (Fig 8c) a radical change occurs due to the increase in the angle of incidence, which is probably a consequence of the bursting of the strake vortex. With blowing quite a large area of secondary separation occurs close to the leading edge outboard of the kink, marked by a narrow region where the tufts point inboard. This secondary separation is largest about $\eta = 0.6$, where there is a marked reduction in the excitation⁽³⁾ downstream of $x/c = 0.3$. The secondary separation also extends to $\eta = 0.8$, where the excitation is increased up to about $x/c = 0.4$ and decreased downstream of $x/c = 0.6$. As expected, with the wing flow dominated by the large, swept separation bubble, scale effects are small.

For $\alpha = 30^\circ$ the flows are essentially similar in character to those observed at $\alpha = 25^\circ$. However now, even without blowing, there is a small area of secondary separation outboard of the kink marked by tufts pointing inboard. This area is increased greatly by blowing. In this

region the tufts are directed inboard with blowing (up to about $x/c = 0.14$ for $\eta = 0.6$ and up to about $x/c = 0.30$ for $\eta = 0.8$). Presumably for $\eta = 0.6$ the secondary separation is smaller and closer to the surface than for $\eta = 0.8$. This might explain the increased excitation in the leading-edge region for $\eta = 0.6$ (Fig 7c) compared to $\eta = 0.8$ (Fig 7d). For the lower speed with blowing the secondary separation is appreciably larger. Somewhat surprisingly, this larger scale separation gives larger suction and higher excitation on the upper surface at $\eta = 0.6$ (Fig 7c) and $\eta = 0.8$ (Fig 7d). This minor anomaly is best attributed to some variation in the momentum coefficient when blowing. It is important to recall that without blowing ($C_{\mu} \equiv 0$) there is no change in either the suction or the excitation when the speed is reduced from $U = 60$ to 40 m/s. Thus without blowing there are no scale effects (cf Fig 7d) on the very large separation shown in Fig 8d.

Special tests at $\alpha = 35^\circ$ and 40°

A severe test of the concept of leading-edge blowing was made by special tests at $\alpha = 35^\circ$ (Fig 9) and 40° . For these very high angles of incidence it was reasonable to assume that, without blowing the vortex burst was close to or at the wing apex (position 1 in Fig 9). Blowing was then applied to the strake, displacing the vortex breakdown position downstream until the fin buffeting was a maximum, with the vortex burst near the fin (position 2). The blowing was then increased further until the fin buffeting reached the lower "plateau" level, with the vortex burst displaced downstream of the fin (position 3).

For $\alpha = 35^\circ$, Fig 9(a) shows that blowing makes only a small increase in the static bending moment coefficient, C_{BF} . However, the level C_{BF} remains low relative to the attached flow values, indicating that local separations about the fin would still degrade the lateral stability relative to that observed below $\alpha = 15^\circ$ (similar remarks apply for $\alpha = 40^\circ$). Figs 9b and 9c show that the fin and wing buffeting first increase to maxima at the vortex burst position 2 and then fall to minima at vortex burst position 3.

For $\alpha = 40^\circ$ similar remarks apply for the control parameters. However, there was evidence that the high blockage at $\alpha = 40^\circ$ was modifying the flow. Hence these results (given elsewhere⁽³⁾) are omitted.

The forces and flow visualisation for $\alpha = 35^\circ$ and 40° give good evidence for the effectiveness of leading-edge blowing (even when this blowing is confined merely to

the strake) on a practical aircraft configuration at high angles of incidence. The overall force measurements (Fig 10) suggests that for these angles of incidence the corresponding small increases in lift coefficient and the large decreases in drag coefficient would largely offset the loss of engine thrust required to provide the requisite values of C_{μ} .

(4) Owen, T.B., "Techniques of pressure fluctuation measurements employed in RAE low speed wind tunnels". AGARD Report 172 (1958)

Crown Copyright Reserved 1994/DRA

Conclusions

Tests on a large half model of an EAP type configuration provided with tangential leading-edge blowing to control flow separation suggest seven conclusions.

- (1) The technique works as well on this large model of a practical aircraft configuration as it has on small models.
- (2) As expected from previous tests on small models, the blowing momentum coefficient, C_{μ} , acts as the primary control of the aerodynamic performance. However, somewhat lower values of C_{μ} appear adequate in the present tests.
- (3) On this wing, for the same value C_{μ} , the uniform slot is more effective than a tapered slot of the same area.
- (4) On this wing, for the same value of C_{μ} , the narrow slot (0.5 mm) is more effective than the wider slot (1 mm).
- (5) Apart from possible scale effects implied for $\alpha = 30^\circ$, no significant scale effects have been noticed in the Reynolds number range from 2.5×10^6 to 4.3×10^6 . No further effects are expected up to say, $R = 30 \times 10^6$.
- (6) This technique should be effective in reducing leading-edge separation on other wings with round leading edges and varying sweep.
- (7) Reduction of leading-edge separation on the strake produces a large reduction in fin buffeting and a smaller reduction in wing buffeting.

References

- (1) Bean, D.E., Greenwell, D.I., Wood, N.J., "Vortex control technique for the attenuation of fin buffet". AIAA J Aircraft, Vol 3 (6), p 847-853 (1993)
- (2) Craig, K., "Computational study of blowing on delta wings at high alpha". AIAA J Aircraft, Vol 3 (6), p 833-839 (1993)
- (3) Mabey, D.G., Pyne, C.R., "Effect of tangential leading-edge blowing on a typical combat aircraft configuration". DRA TR 93-013 (1993)

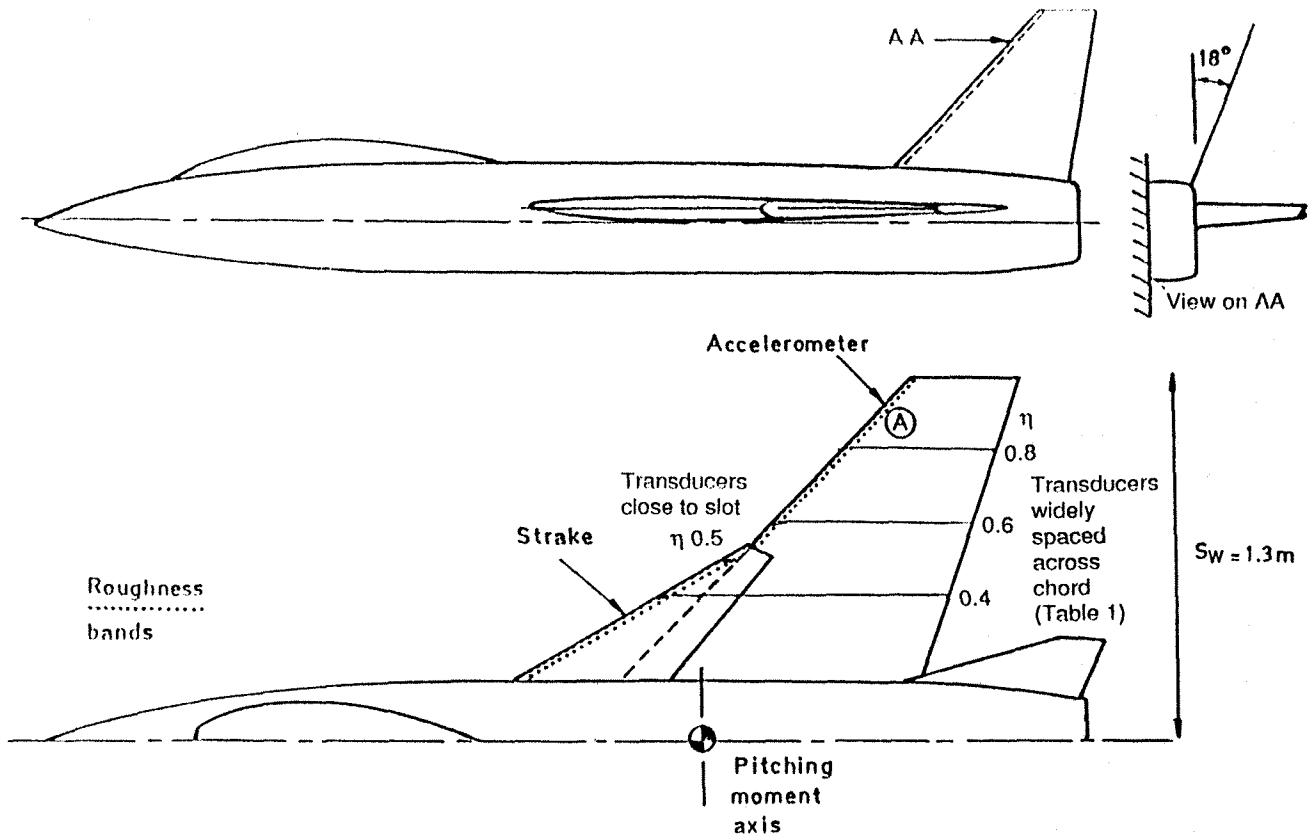
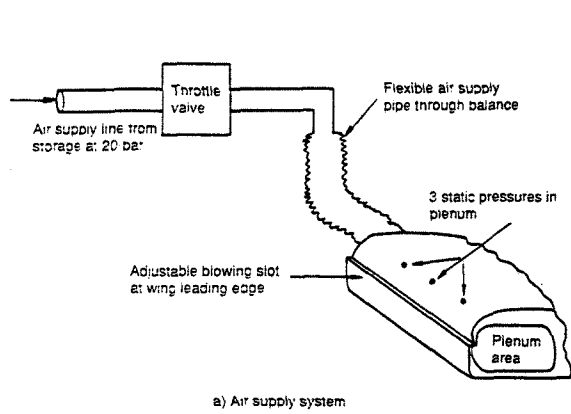
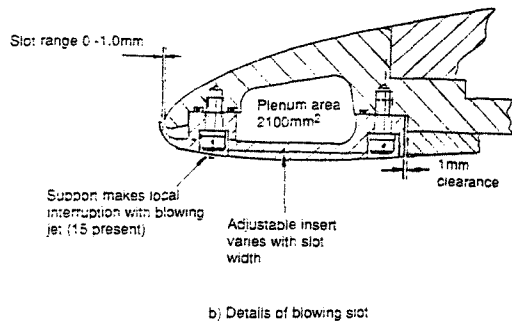


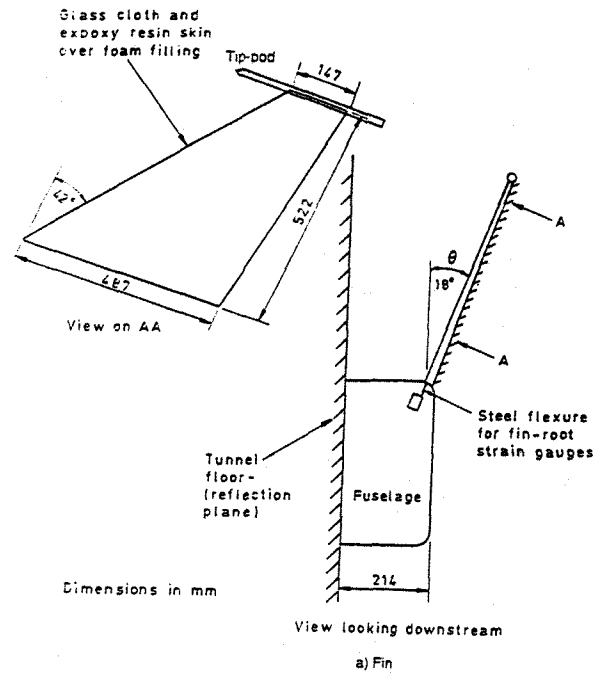
Fig 1 GA of model



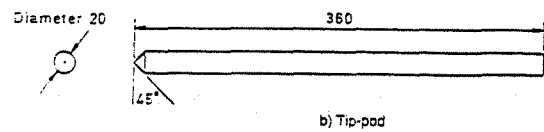
a) Air supply system



b) Details of blowing slot



a) Fin



b) Tip-pod

Fig 2 Air supply and blowing slot

Fig 3 Fin and tip-pod

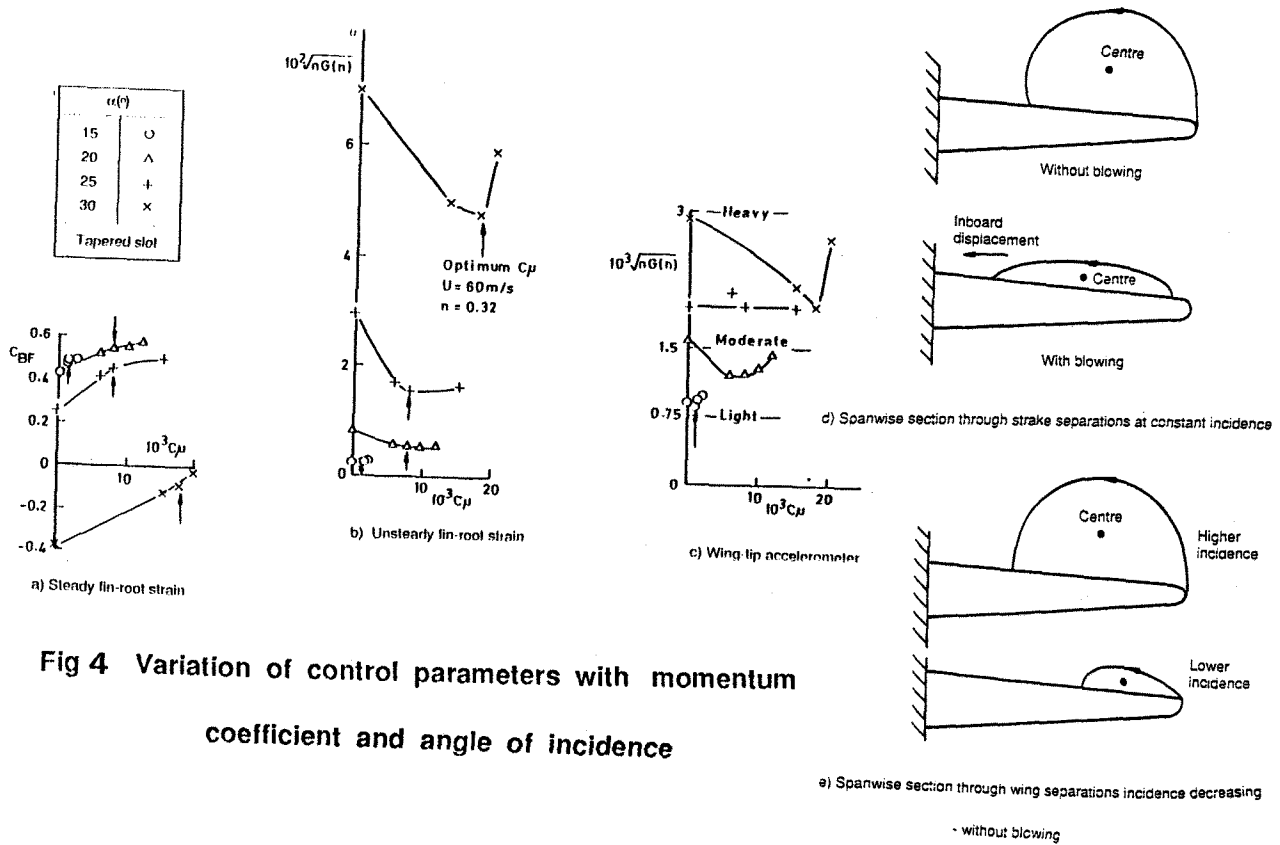


Fig 4 Variation of control parameters with momentum coefficient and angle of incidence

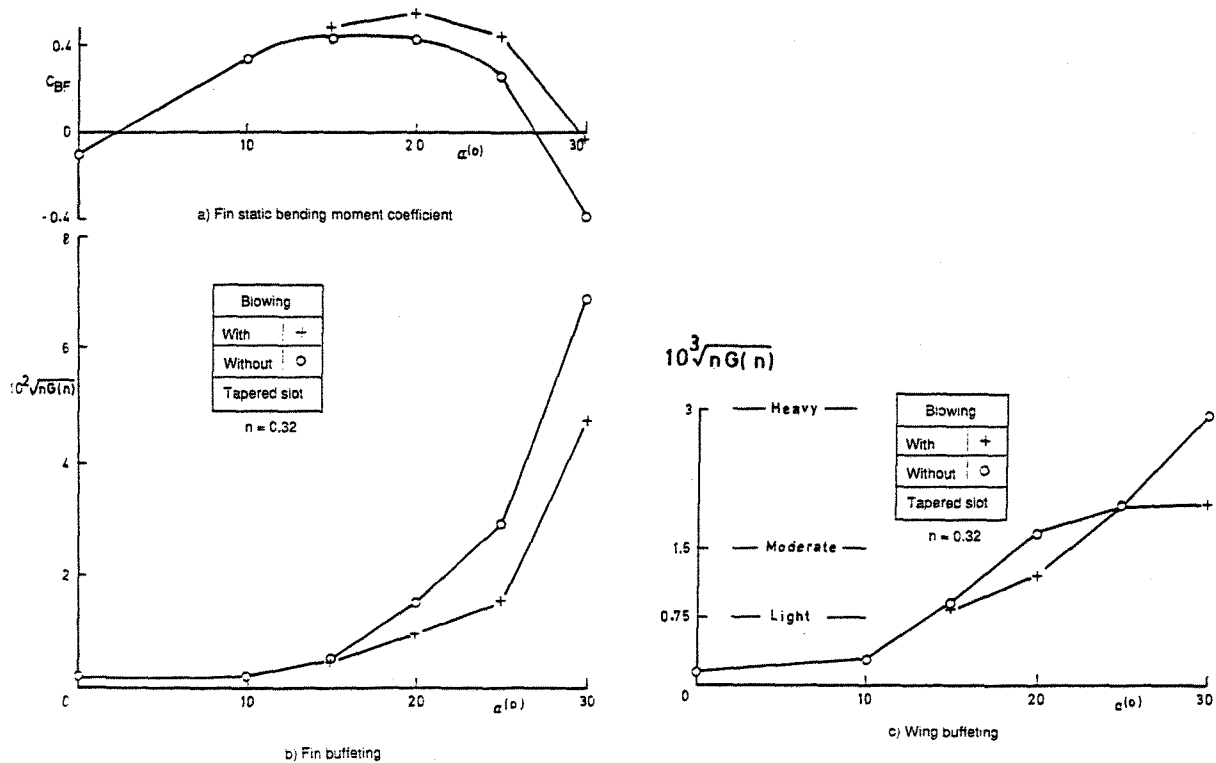


Fig 5 Variation of control parameters with optimum C_{μ} and angle of incidence

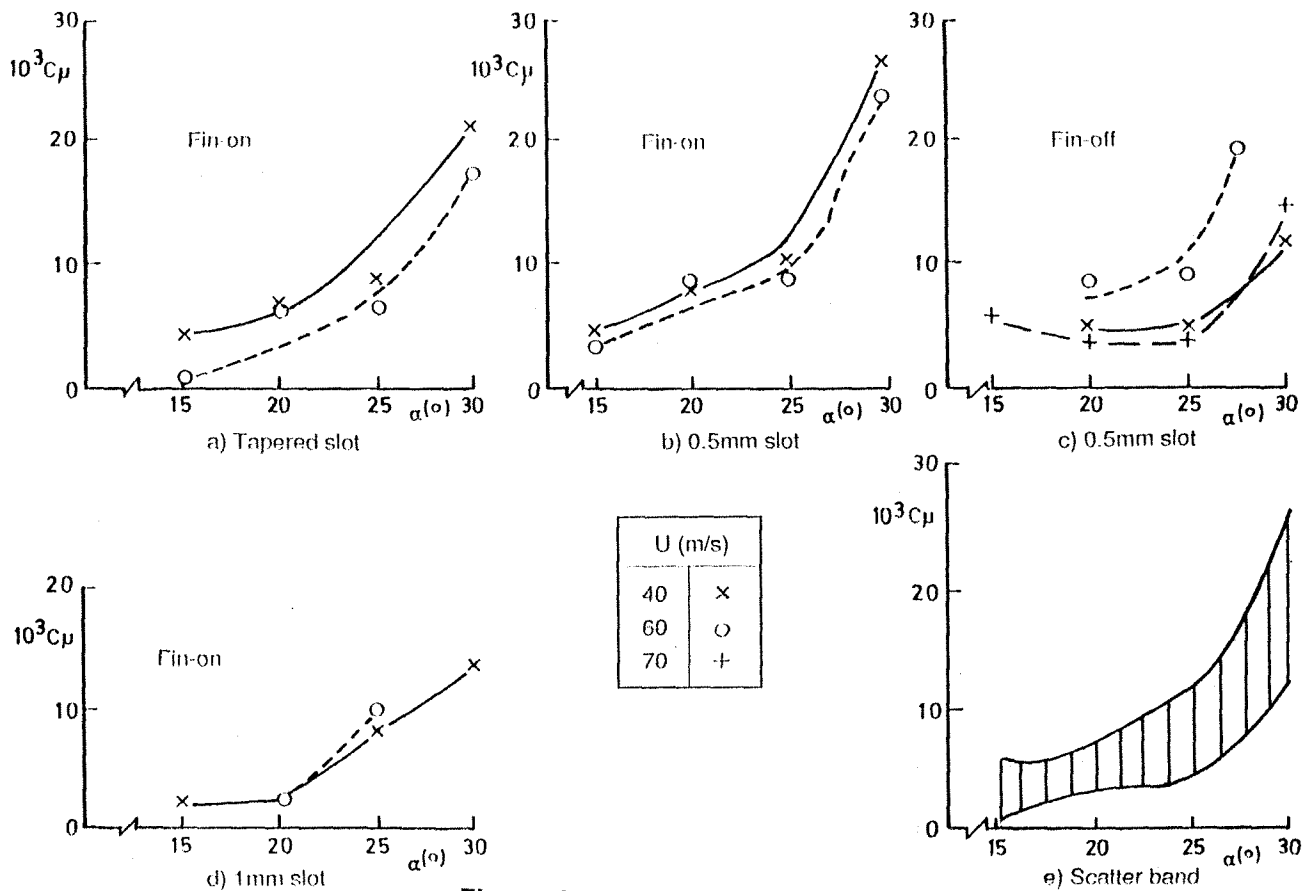


Fig 6 Optimum momentum coefficients

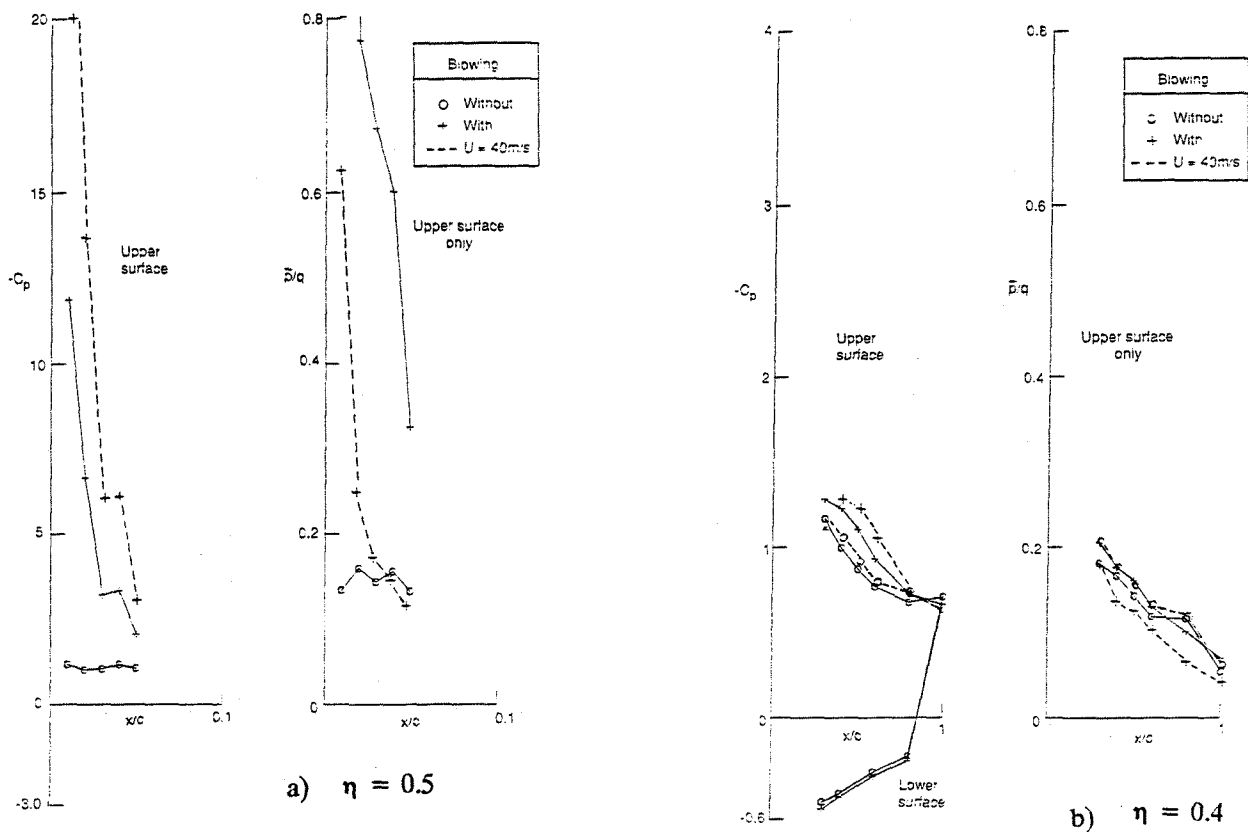


Fig 7 Pressure distributions for $\alpha = 30^\circ$

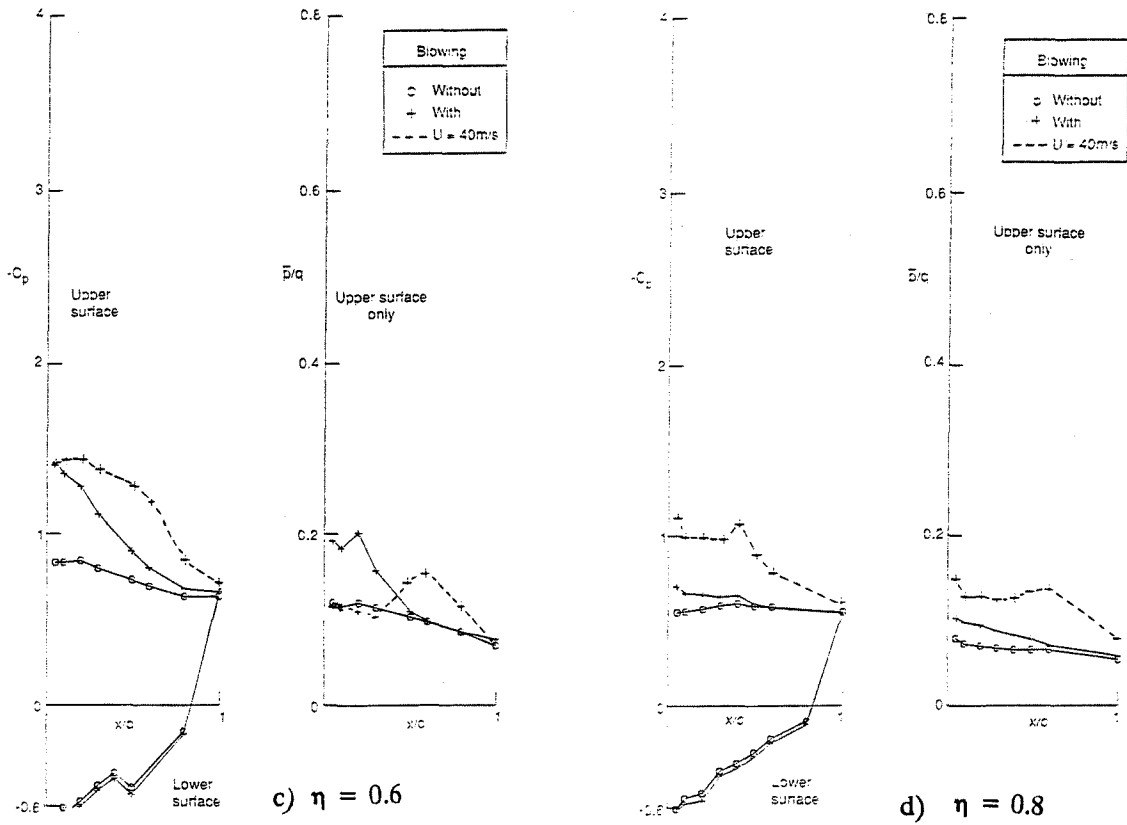


Fig 7 $\alpha = 30^\circ$ (concl'd)

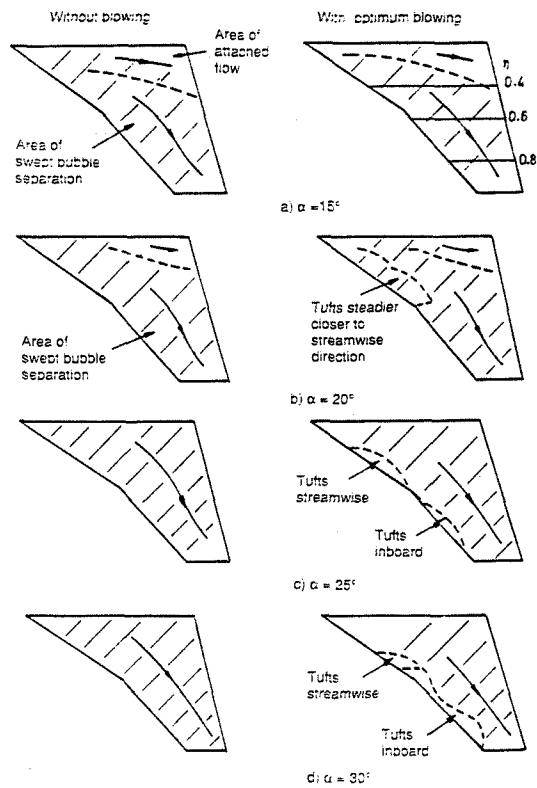


Fig 8 Effect of optimum blowing on mini-tuft photographs

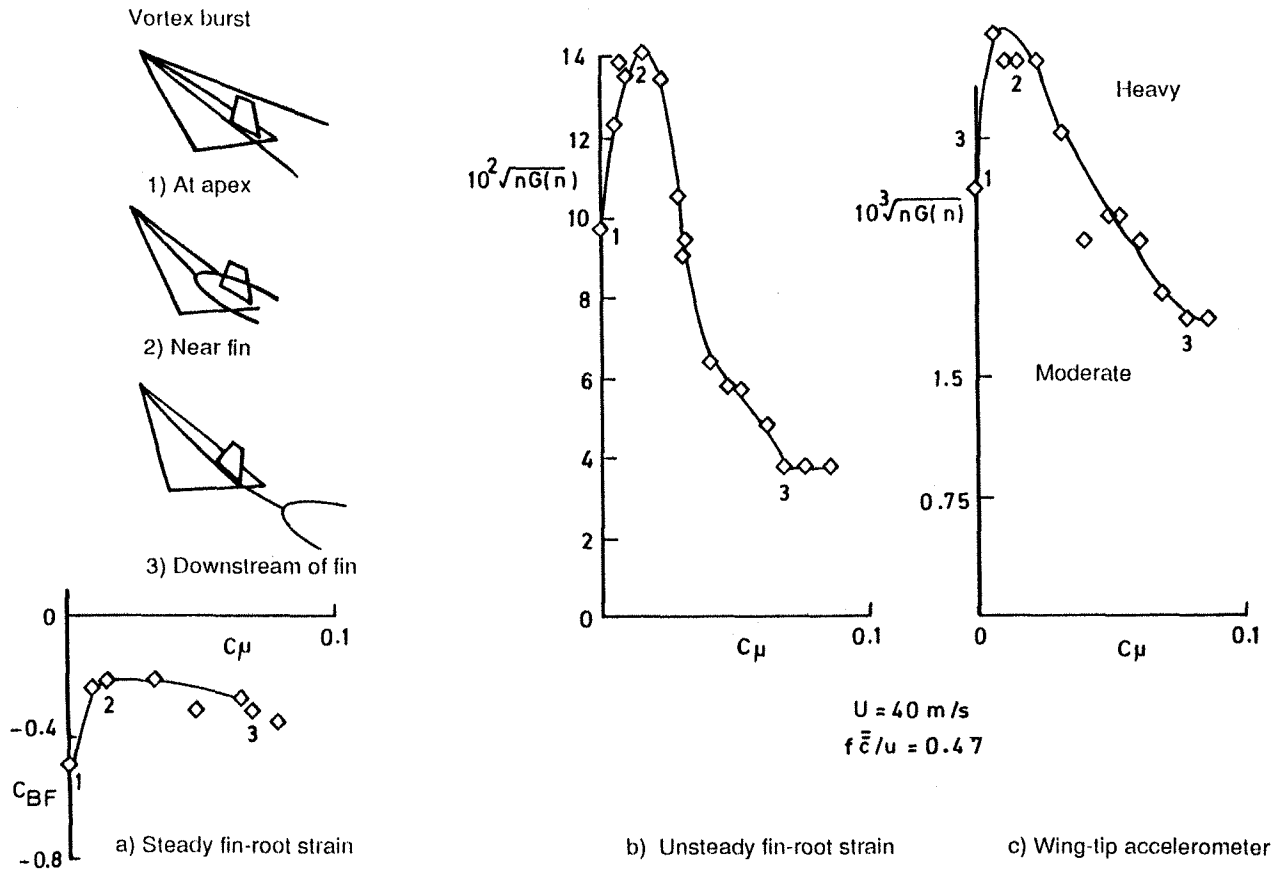


Fig 9 Variation of control parameters and mini-tuft photographs with momentum coefficient $\alpha = 35^\circ$

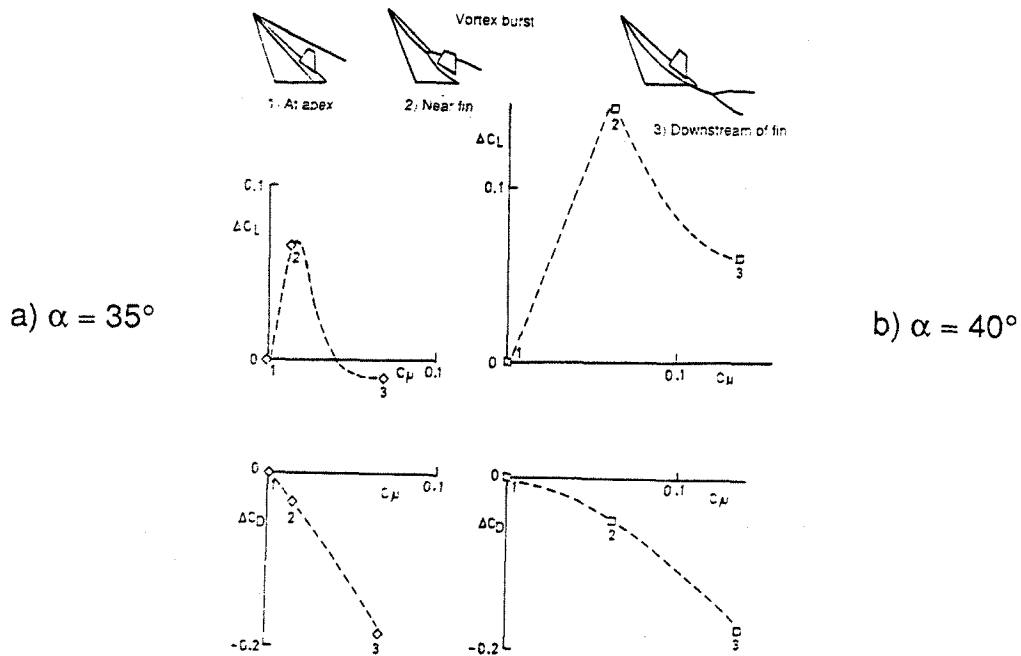


Fig 10 Variation of incremental force coefficient with momentum coefficient